Reduced-Order Modelling of Switched/Inductor-Capacitor Based High Gain Converter for Fuel Cell Application

Sumathy Ponnuswamy*, Divya Navamani Jayachandran*‡, Lavanya Anbazhagan*

*Department of Electrical and Electronics Engineering, SRM Institute of Science and Technology, Kattankulathur, India

‡Corresponding Author; Divya Navamani Jayachandran, Department of Electrical and Electronics Engineering, SRM Institute of Science and Technology, Kattankulathur, India.

email: divyanaj@srmist.edu.in

Received: 14.01.2022 Accepted: 27.02.2022

Abstract- Many state variables are resulted from a high gain power converter due to the presence of many passive components to describe the dynamic system. This results in complex higher order differential equations. To achieve the objective of designing the controller for the power converter with reduced time and in ease, the necessity of order reduction of the system. This paper presents the pole clustering technique for high gain converter to obtain a reduced order for the polynomial of the model, in terms of simple mathematical calculation. The characteristics of the higher order system are presented and it remains the same obtained from the reduced order system. Before carrying out the reduced order model, it is necessary to derive the transfer function of the converter. The derivation of small signal open loop model of suggested high gain power converter is carried out by applying switching flow graph with Mason's gain formula. MATLAB simulation results are also presented to aid the sustainability of investigation. Finally, the experimental results of the selected high gain converter are presented for validation.

Keywords Fuel cell, high gain, pole clustering, reduced-order, switching flow graph

Nomenclature

HGSIC - High gain switched inductor-capacitor
PEM - Proton Exchange Membrane
V_{FC} - Fuel cell voltage
η_{act} - Activation overpotential
η_{ohm} - Ohmic overpotential
ηcon - Concentration overpotential.
SFG - Signal flow graph
K - Number of poles
C_X - Cluster centre
ψ_j - Improved cluster centre
$N_{R(S)}$ - Numerator polynomial
$D_{R(S)}$ - Denominator polynomial

1. Introduction

Fuel cell is booming very rapidly in all fields especially in electric vehicle application. It is a device which produce electricity through electrochemical reaction and it unceasingly produces the energy as long as hydrogen is provided. Fig 1 present the structure of fuel cell with the layers of Proton Exchange Membrane (PEM) fuel cell. In this electrochemical conversion device, the by products are water and heat. It uses oxygen and hydrogen to yield electricity. Since it uses only pure hydrogen fuel as the input, it is a clean and carbon-free device. The efficiency of the system can be further improved by combining the device with other power system to utilizes the fuel cell's waste heat for further process. The dynamic model of fuel cell stack is obtained by a mathematical approach. The fuel cell voltage in steady-state condition is presented as

$$V_{FC} = V_{rev} - \eta_{act} - \eta_{ohm} - \eta_{con} \quad (1)$$

Where ηact is activation overpotential, ηohm is ohmic overpotential and ηcon is concentration overpotential.

Simultaneously, the steady-state fuel cell characteristics is presented in Fig 1 where the reversible voltage (Vrev) is combined with the overpotentials. The dynamics of the fuel cell can be studied with the dynamic equivalent circuit model and it is presented in Fig 1. The dynamic of the fuel cell can be modelled as the capacitor which represents the charge double layer and a combination of series (Rs) and parallel (Rp) resistor.

The representation of higher order system poses a difficulty in design of control system for control of a physical system control. Owing to cost effective implementation of higher order systems, it is desirable to replace the same with reduced order one while the properties of actual higher order system being maintained qualitatively. Analysing DC-DC converter by exploring its transfer function is one of the easiest ways. For this analysis, a mathematical model of the converter has to be obtained. Linearization and averaging are important methods to model and explore a converter to investigate its frequency response.

Literature provides several techniques of order reduction, satisfying the advantage of simplified model stability and retention of original system basic physical properties [1]-[4]. Composite order reduction techniques with numerator polynomial order reduced by Pade approximation, continued fraction expression, Chebyshev polynomial series and cuckoo optimization and denominator order reduced by Routh Hurwitz, pole clustering genetic algorithm technique and is presented in [5]-[10]. The numerical examples provided validate the techniques proposed. One of the prominent errors in analysis of converter is integral square error (ISE). The response of the higher and lower order systems is compared and proved for minimal ISE which is taken as the function of objective. The sensitivity of the Pade approximation is shown to be reduced with a suitable combination of Pade technique and Fourier transformation. It is shown to be improved in [11]-[13]. Without introducing complexity in addition, Pade approximation is compared to be better with that of x-parameter model for a model based on frequency domain [14]. An exponential function expression obtained thorough restrictive Pade approximation and also discussion on some of its algebraic properties is presented in [15].

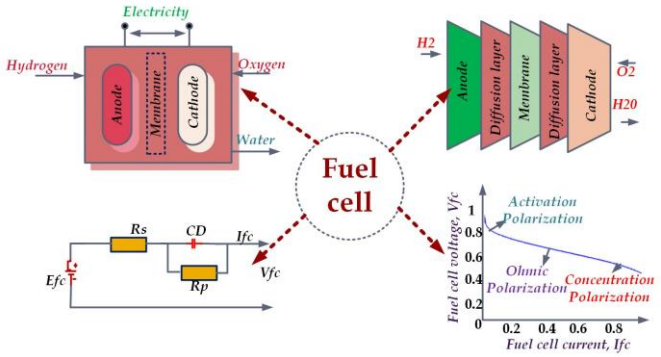

Fig. 1. Basics of fuel cell

A dynamic system control be analysed using Model Reduction Approximation and found to preserve original transfer function characteristics. A comparison between the new approximation method and other order reduction method are presented with appreciable remarks [16]. H_2 norm principle is shown to be an approximation satisfactory with respect to stable linear discrete time systems. The results are presented for validity illustration of the method pro-posed [17]. A novel Pade approximation is presented with deeper analysis of the method along with the pole placement concept [18]. An eight-order system is reduced using mixed Pade approximation and a modified pole clustering technique is given in [19] and shown to have efficient stability when compared with other mixed approximation techniques. Reduction of H∞ model is given in [20] along with the implementation of cone complementary algorithm of linearization.

Another Pade type system order reduction approximation is presented in [21] and correctness of system is illustrated. Apart from algebraic loops a new loop reversal rule is proposed in [22] to signal flow manipulation which is still missing out in textbooks. Luo converter is investigated using Manson's gain formula and signal flow graph, frequency response and sustainability of the converter is investigated using MATLAB simulation shown [23]. Derivations of any order can exactly be calculated using signal flow graphs. The complexity of the calculations is shown to be highly reduced in the approach presented [24]. The coefficients of numerator and denominator orders are reduced to the desired order. Harmonic linearization method complemented by the signal flow graphs is presented in [25]. Complicated phase locked loops are modelled using signal flow graphs and results for the two number of single-phase locked loops are presented. For complex system diagnosis, a new multi-signal modelling is proposed with step-by-step procedure and validated with case study [26].

For a DC-DC structure with single inductor triple output, a unified signal flow graph (SFG) is developed and by comparing SFG model and hardware results, the modelling errors are observed and presented [27]. An adaptive voltage regulation of a dual input boost converter is designed for load of unknown values. The reference inductor currents are computed in terms of load conductance. Using FPGA, the controls are implemented and presented [28]. Negative feed-back employed switching supplies are over viewed using SFG for a DC-DC converter in both discontinuous and continuous mode of operation and its analysis is presented in detail [29]. An approach based on transform matrix the SFG loop gain is analysed and given in [30]. A key to the transfer function of the topology is derived by reduced redundant power processing technique and signal flow modelling is given. This method is observed to be an easier method for transfer function derivation of a converter and is given in [31].

In this paper, attention is focused on system specifications with minimal ISE. With the objective of same steady state parameters of original and reduced order systems, the steady-state error, rise time, peak time and settling time are analysed and the results are presented. Hence a composite method of order reduction, with coefficient matching technique for numerator polynomial and modified pole clustering technique for denominator polynomial is applied for the high gain converter transfer function. The major contributions of this research are

- To steady the dynamic analysis of High gain switched inductor-capacitor (HGSIC) converter.
- To provide an analytical approach to obtain the transfer function of high gain boost converter by application of signal flow graph method and Mason's gain formula.
- To reduce the order of the converter to ease the design of controller for this topology.
- To validate the operation of the topology with experimental study.

This paper is organized as follows: section 2 is dedicated to explain the role of fuel cell in future transportation system and the significance of power converter. The methodology incorporated for this study is briefed in section 3. Section 4 exclusively devoted for switching flow graph modelling. Higher dimensional converter is analysed with reduced-order modelling and the illustration is presented in section 5. Section 6 presents the voltage gain and efficiency analysis. Section 7 is devoted to the discussion on experimental study. Finally, the topology's performance is concluded in section 8.

2. Application of Fuel Cell

All In the past few years, many kinds of research have been done and with all the results obtained, observed that fuel cell has the potential to become an ultimate power source in upcoming years. Fuel cells can be used for portable, backup, transportation, and stationary power applications. Fig 2 depicts the several applications of fuel cells, and it is noticed that the fuel cell is slowly intervening in future power engineering.

Fig. 2. Various application of fuel cell

Compared to an IC Engine vehicle, a fuel cell vehicle is more efficient and eco-friendlier. Due to the fuel cell's high storage capacity, a large range of automobiles can be operated. Generally, a vehicle that is powered by a fuel cell needs a DC-DC converter. It is done to connect the HV bus powered by a fuel cell with the lower voltage bus with the auxiliary loads. With the use of fuel cells, we need a storage device to store energy obtained by regenerative braking, as this is out of the fuel cell's capacity. It gives an advantage rather than charging from the control method because, in the control method, we can charge only when it falls below 50 %. Hence it reduces the efficiency and performance of the fuel cell vehicle when compared to regenerative braking. To avoid overstressing, mechanical braking can be used in the vehicle.

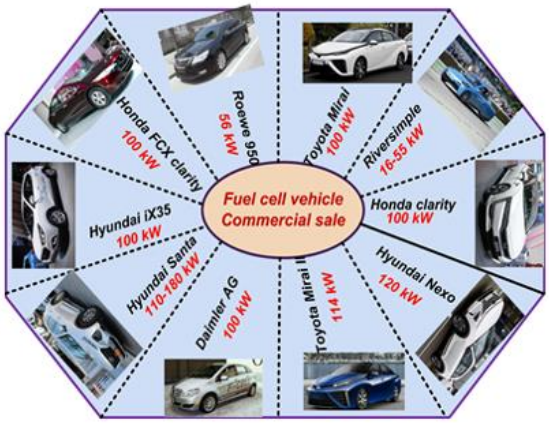

Fig. 3. Commercially marketed fuel cell vehicle

Though there is an alternative way, a vehicle battery attached to the dc-dc converter can be used for this purpose. Apart from this, an ultracapacitor can be used for storing power. In this paper, different dc-dc converters topologies are used to generate the output and compare them with the other one. As high gain converter technology is used, the HV bus can be boosted up to 300 V by drawing it from the vehicle's battery. As we know that a vehicle does not move at a uniform speed, it has braking and acceleration requirements to regulate its speed. So, there is a need to change the load quickly for better transmission. The commercially marketed fuel cell powered cars in the market from 2001-2020 is depicted in the Fig 3.

It is observed in the literature, the hydrogen fuel is more efficient and four times more expensive compared to gasoline and diesel. Hydrogen refilling stations for fuel cell powered vehicle is available world-wide whereas the number of these stations are very less compared to gasoline filling station. In India, this hydrogen powered fuel cell is still in research and development stage. Fuel cell application require unidirectional power converter with high gain because the fuel cell provides low voltage. The High gain switched inductor-capacitor converter is more suitable for this application and it can retrofit to the power converter available in the conventional vehicle.

3. Methodology

In this article, a high gain dc-dc converter is proposed with dynamic study for fuel-cell application. Fig 4 (a) presents the methodology followed to reduce the order of the converter. This is carried out by modelling the converter with switching flow graph. The topology considered for this dynamic analysis is presented in Fig 4 (b). Switched-inductor/capacitor integrated boost converter is selected due to the presence of higher number of passive components.

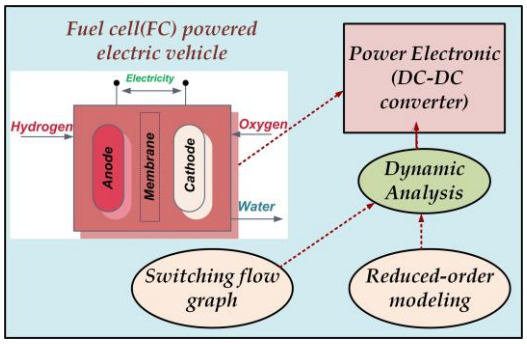

(a)

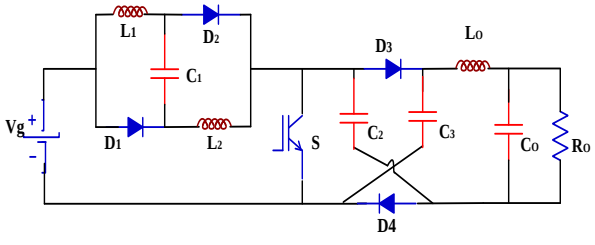

(b)

Fig. 4. (a) Methodology (b) High gain switched inductor-capacitor (HGSIC) converter circuit

4. Signal flow graph modelling

Modelling of the proposed dc-dc converter is obtained through the signal flow graph approach. The switching devices are assumed ideal and ESR values are neglected. The Signal flow graph of the proposed converter with the perturbated state variables as capacitor voltage and inductor current is presented. The small and large-signal parameters of the proposed converter is modelled and based on the loop analysis the transfer function is derived. Moreover, small signal dynamic behaviour of the converter is presented for input voltage and duty cycle.

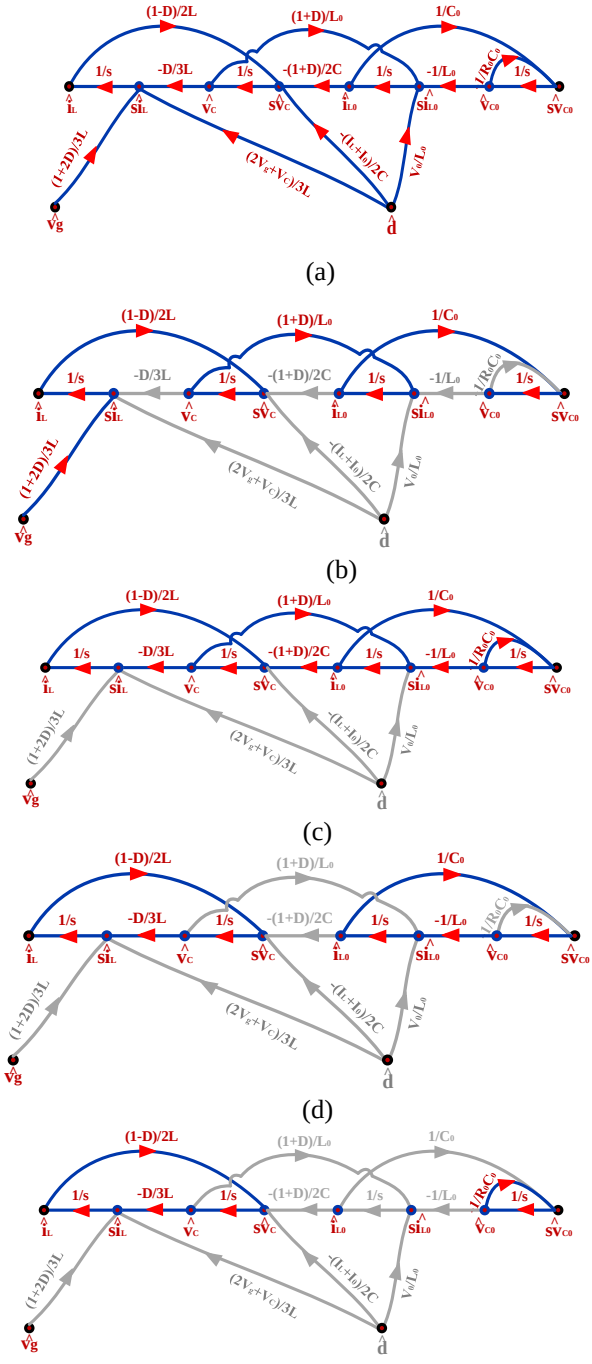

Fig. 5. (a) Signal flow graph (SFG) of proposed converter (b)-(f) SFGs for determining input to output transfer function marketed fuel cell vehicle

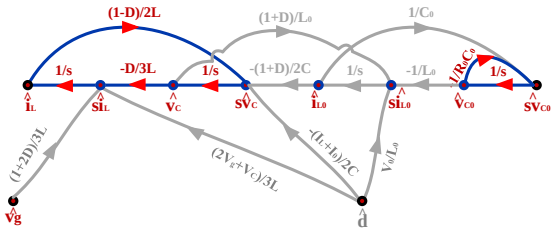

(f)

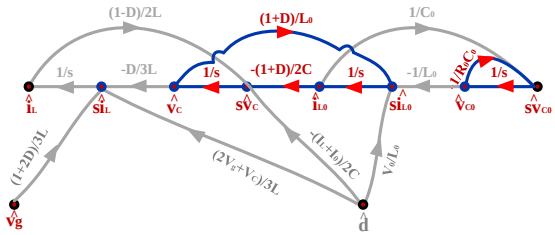

(g)

Fig. 6. (a)-(g) SFGs for determining duty cycle to output transfer function

Fig 5 is utilized to determine the transfer function given below with the help of Mason's gain formula. By simplifying and rearranging, the input to output transfer function is obtained as

$$\frac{V_0(s)}{V_g(s)} = \frac{\frac{(1-D)(1+2D)D'}{6LL_0CC_0}}{\frac{S^4 6LL_0CC_0R_0+S^3 6LL_0C+S^2[D'^2L_0C_0R_0+(1+D)^2 3LC_0R_0+6LCR_0]+S[D'^2L_0+(1+D)^2 6L]+R_0D'^2}{6LL_0CC_0R_0}} \quad (1)$$

Fig 6 is drawn to determine the duty cycle to output transfer function. Table 1 and 2 present the forward path gain for determining the transfer function of input to output and duty cycle to output respectively.

Table 1. Appearance properties of accepted manuscripts

S.No.	Variables	Forward Path Nodes	Forward Path Gain
1	P	$\widetilde{v_g} \to s\widetilde{i_{L1}} \to \widetilde{i_{L1}} \to s\widetilde{v_C} \to \widetilde{v_C} \to s\widetilde{i_{L0}} \to \widetilde{i_{L0}} \to s\widetilde{v_{C0}} \to \widetilde{v_{C0}}$	$\frac{[1-D]1+D][1+2D]}{6s^4LL_0CC_0}$
2	C_1	$s\widetilde{i_{L1}} \to \widetilde{i_{L1}} \to s\widetilde{v_C} \to \widetilde{v_C} \to s\widetilde{i_{L1}}$	$\frac{-[1-D]^2}{6s^2LC}$
3	C_2	$s\widetilde{i_{L0}} \to \widetilde{i_{L0}} \to s\widetilde{v_{C0}} \to \widetilde{v_{C0}} \to s\widetilde{i_{L0}}$	$\frac{-[1+D]^2}{2s^2L_0C}$
4	C_3	$s\widetilde{i_{L21}} \to \widetilde{i_{L21}} \to s\widetilde{v_{C1}} \to \widetilde{v_{C1}} \to s\widetilde{i_{L21}}$	$\frac{-1}{s^2L_0C_0}$
5	C_4	$s\widetilde{v_{C0}} \to \widetilde{v_{C0}} \to s\widetilde{v_{C0}}$	$\frac{-1}{sR_0C_0}$
6	C_1 C_3	Non-touching loop pair gain	$\frac{[1-D]^2}{6s^4LL_0CC_0}$
7	C_1 C_4		$\frac{[1-D]^2}{6s^3LR_0CC_0}$
8	C_2 C_4		$\frac{[1+D]^2}{2s^3L_0R_0CC_0}$

Table 2. Forward path gain for determining duty cycle to output transfer function

S.No.	Variables	Forward Path Nodes	Forward Path Gain
1	P_1	$\tilde{d} \to s\widetilde{i_{L1}} \to \widetilde{i_{L1}} \to s\widetilde{v_C} \to \widetilde{v_C} \to s\widetilde{i_{L0}} \to \widetilde{i_{L0}} \to s\widetilde{v_{C0}} \to \widetilde{v_{C0}}$	$\frac{-[2V_g+V_c][1-D]1+D]}{6s^4LL_0CC_0}$
2	P_2	$\tilde{d} \to s\widetilde{v_C} \to \widetilde{v_C} \to s\widetilde{i_{L0}} \to \widetilde{i_{L0}} \to s\widetilde{v_{C0}} \to \widetilde{v_{C0}}$	$\frac{-[I_L+V_c][1-D]1+D]}{6s^4LL_0CC_0}$
3	P_3	$\tilde{d} \to s\widetilde{i_{L0}} \to \widetilde{i_{L0}} \to s\widetilde{v_{C0}} \to \widetilde{v_{C0}}$	$\frac{V_c}{s^2L_0C_0}$
4	Δ_1	Applied to loops not touching the respective forward paths mentioned above	$\Delta_1=\Delta_2=1$
5	Δ_3		$1+\frac{[1-D]^2}{6s^2LC}$
6	C_1	$s\widetilde{i_{L1}} \to \widetilde{i_{L1}} \to s\widetilde{v_C} \to \widetilde{v_C} \to s\widetilde{i_{L1}}$	$\frac{-[1-D]^2}{6s^2LC}$
7	C_2	$s\widetilde{i_{L0}} \to \widetilde{i_{L0}} \to s\widetilde{v_{C0}} \to \widetilde{v_{C0}} \to s\widetilde{i_{L0}}$	$\frac{-[1+D]^2}{2s^2L_0C}$

8	C_3	$si_{\widetilde{L21}} \rightarrow i_{\widetilde{L21}} \rightarrow s\widetilde{v_{C1}} \rightarrow \widetilde{v_{C1}} \rightarrow si_{\widetilde{L21}}$	$\frac{-1}{s^2 L_0 C_0}$
9	C_4	$s\widetilde{v_{C0}} \rightarrow \widetilde{v_{C0}} \rightarrow s\widetilde{v_{C0}}$	$\frac{-1}{sR_0 C_0}$
10	C_1 C_3	Non-touching loop pair gain	$\frac{[1-D]^2}{6s^4 LL_0 CC_0}$
11	C_1 C_4		$\frac{[1-D]^2}{6s^3 LR_0 CC_0}$
12	C_2 C_4		$\frac{[1+D]^2}{2s^3 L_0 R_0 CC_0}$

Fig 6 is utilized to determine the transfer function given below with the help of Mason's gain formula. By simplifying and rearranging, the duty cycle to output transfer function is obtained as

$$\frac{V_0(s)}{d(s)} = \frac{\frac{(2Vg+Vc)(1-D)D' + Vc(D'^2 + 6S^2L^2) - 3S^2L(IL + I0(1+D))}{6LL_0CC_0}}{\frac{S^4 6LL_0CC_0R_0 + S^3 6LL_0C + S^2[D'^2 L_0C_0R_0 + (1+D)^2 3LC_0R_0 + 6LCR_0] + S[D'^2 L_0 + (1+D)^2 6L] + R_0D'^2}{6LL_0CC_0R_0}} \quad (2)$$

(1) and (2) show the transfer function for the full order system determined using Mason's gain formula illustrating the characteristics of the proposed converter.

5. Reduced order modelling

There are several algorithms proposed for order reduction of the system by retaining the characteristics of the system like Pade approximation, pole-clustering etc. In this section, pole clustering is applied to reduce the four orders to two order system and the steps involved in the algorithm are elaborated in detail. There are 2 steps in model reduction in the method proposed.

5.1. Generalized algorithm of pole clustering technique

Pole clustering technique is used to obtain the reduced order of the denominator polynomial [36]. From the given higher order denominator polynomial calculates the 'n' number of poles. The reduced system order is equal to the number of cluster centres. Pole distribution is made in such a way that the cluster centre has no repetition of poles. At least one pole should be distributed to each of the cluster center. The maximum number of poles distributed to each of the cluster centers is not limited. Let the available number of poles in the cluster center be 'K'. P_1, P_2, P_3 -----P_K are the poles. The poles are arranged in such a manner that$|P_1| < |P_2| < |P_3| - - - - - |P_K|$.

Using the procedure below the reduced order system cluster center can be found.

Procedure:

1. Let the total number of poles be K, such that$|P_1| < |P_2| < |P_3| - - - - - |P_K|$.
2. X=1 is set.
3. The pole cluster is given as
$$C_X = \left[\left(-\frac{1}{|P_1|} + \sum_{i=2}^{K} \frac{-1}{|P_i - P_1|}\right) \div K\right]^{-1} \quad (3)$$
4. Check whether X=K, if X=K, then stop process and the cluster centre finally is C_E=C_X. Else proceed to next step.
5. Set X=X+1
6. The cluster centre improved value is
$$C_X = \left[\left(-\frac{1}{|P_1|} + \frac{-1}{C_X}\right) \div 2\right]^{-1} \quad (4)$$
7. Check whether X=K. If yes, then C_E=C_X else move to step 5.

Let the 'n' order original higher order discrete time system transfer function be

$$G(S) = \frac{N(S)}{D(S)} = \frac{Q_0 + Q_1 S + Q_2 S^2 + - - - - - - - + Q_e S^e}{P_0 + P_1 S + P_2 S^2 + - - - - - - - + P_v S^v} \quad (5)$$

Where e≤v.

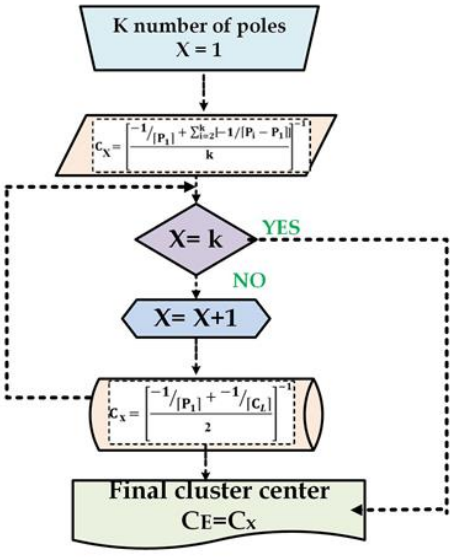

Fig. 7. Improved pole clustering procedure

Step-1: - Determination of denominator polynomial reduced order using an improved pole clustering technique [36].

Let the form of single input single output time variant linear system higher order transfer function be

$$G(S) = \frac{U_0+U_1S+U_2S^2+--------+U_{H-1}S^{H-1}+U_HS^H}{V_0+V_1S+V_2S^2+ --------+V_{W-1}S^{W-1}+V_WS^W} \quad (6)$$

Where H≤W, and G(S) is,

$$G(S) = \frac{\sum_{j=0}^{m} U_jS^j}{\sum_{j=0}^{n} V_jS^j} = \frac{N(S)}{D(S)} \quad (7)$$

The reduced order correspondingly should be in the form of

$$G_R(S) = \frac{A_0+A_1S+A_2S^2+--------+A_{q-1}S^{q-1}+A_qS^q}{B_0+B_1S+B_2S^2+ --------+B_{r-1}S^{r-1}+B_rS^r} \quad (8)$$

Where q≤r

$$G_R(S) = \frac{\sum_{i=0}^{q} A_iS^i}{\sum_{i=0}^{r} B_iS^i} = \frac{N_R(S)}{D_R(S)}$$

For the same inputs, the responses of the reduced model approximate the original system important characteristics closely. The following three cases are considered for calculating the cluster centre values. On considering the following three cases, the cluster centres can be calculated.

Case-1:- All real denominators poles:

The denominator polynomial of reduced order can be obtained as,

$$D_R(S) = (S + C_{E1})(S + C_{E2}) \dots . (S + C_{Er}) \quad (9)$$

The improved cluster values are $C_{E1}, C_{E2} \dots \dots C_{Er}$ of the order 'r'.

Case-2: - Complex poles:

In a X[th] cluster, let there be 'g' pair of complex conjugate poles as,

$$\left[(\alpha_1 \pm j\beta_1), (\alpha_2 \pm j\beta_2), (\alpha_3 \pm j\beta_3), \dots . \left(\alpha_g \pm j\beta_g\right)\right] \quad (10)$$

Where (g=K/2) and $|\alpha_1| < |\alpha_2| < |\alpha_3| \dots \dots |\alpha_g|$.

To obtain improved clusters respectively, algorithm proposed is applied individually for the imaginary and real parts.

The form of the improved cluster center is

$$\psi_j = \gamma_j \pm j\lambda_j \quad (11)$$

γ_j and λ_j are the values of improved pole cluster respectively for the real and imaginary parts. The denominator polynomial obtained correspondingly is

$$D_R(S) = (S + |\varphi_1|)(S + |\varphi_2|) \dots \dots \left(S + \left|\varphi_j\right|\right) \quad (12)$$

Where j=r

When a reduced model with odd order is required, the 'r' value is to be an odd number.

Case – 3:- If poles are both real and complex in nature:

The improved clustering algorithm is applied separately for complex and real poles to obtain cluster centers. Then the denominator polynomial of reduced order is obtained by combining the complex and real improved cluster poles together.

Step – 2:- Determination of Reduced-order numerator polynomial

The general form of transfer function of the system with reduced order is equated to the general form of transfer function of the higher order systems given. The coefficients of the reduced order system are obtained utilizing the step-1.

$$\frac{h_0+h_1S+h_2S^2+\cdots+h_{p-1}S^{p-1}+h_pS^p}{l_0+l_1S+l_2S^2+\cdots\ldots\ldots\ldots+l_{y-1}S^{y-1}+l_yS^y} \quad (13)$$

$$\frac{w_0+w_1S+w_2S^2\pm\cdots\ldots\ldots+w_{n-1}S^{n-1}+w_nS^n}{t_0+t_1S+t_2S^2+\cdots\ldots\ldots\ldots+t_{m-1}S^{m-1}+t_mS^m} \quad (14)$$

On comparing both sides power 'S' and cross multiplying the equation above, the following equations are obtained.

$h_0t_0 = l_0w_0$
$h_0t_1 + h_1t_0 = l_0w_1 + l_1w_0$
$h_0t_2 + h_1t_1 + h_2t_0 = l_0w_2 + l_1w_1 + l_2w_2$
.
.
.
$h_pt_m = l_yw_n$ (15)

The coefficients $w_0, w_1, w_2, \dots\dots w_n$ can be found by solving the above equations. The form of the numerator polynomial of the reduced order system is as follows.

$$N_R(S) = t_0 + t_1S + t_2S^2 + \cdots + t_{m-1}S^{m-1} + t_mS^m \quad (14)$$

5.2. *Application of Pole clustering to HGSIC converter*

The specification chosen to carry out this study is presented in Table 4.

Table 4. Specification and parameters of HGSIC converter

P=100W	$I_{L0}=I_0=1.3A$
$V_g=12V$	$L_1=L_2=10\mu H$
$V_O=72V$	C=6 µF
$R_O=52\Omega$	$C_0=10$ µF
$I_O=1.38A$	$L_0=100$ µH
D=0.5	$I_{L0}=I_0=1.3A$

The transfer function is obtained as,

$$G(S) = \frac{V_0(S)}{V_g(S)} = \frac{3.75*10^{14}}{S^4+1.9*10^3S^3+3.1*10^9S^2+2.1*10^{12}S+4.17*10^{17}}. \quad (16)$$

The poles of the denominator polynomial of higher-order dimensional HGSIC converter are,

S=-324.6±j11868.36 and -635.33±54385.73 (17)

On application of pole clustering improved method, the cluster poles of reduced-order converter are obtained as,

$\psi 1 = -320.28 + j15784.81$

$\psi 2 = -320.28 - j15784.81$

The reduced order transfer function is obtained as,

$$G_R(S) = \frac{N_R(S)}{D_R(S)} = \frac{226.87*10^3}{S^2+659.38S+252.28*10^6} \quad (18)$$

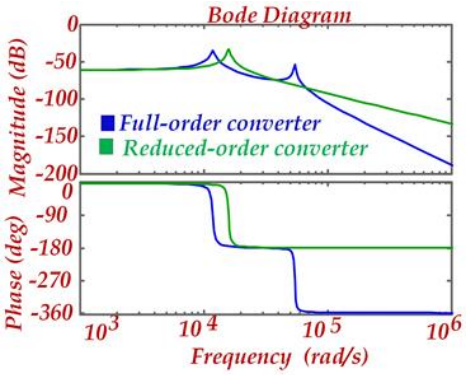

(a)

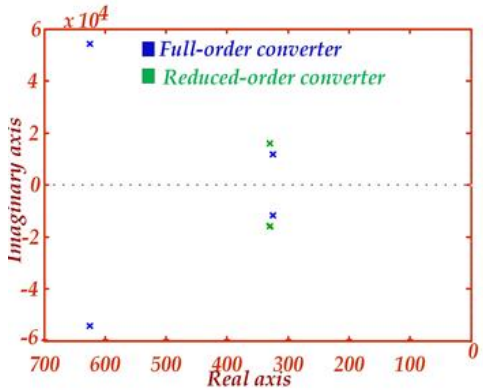

(b)

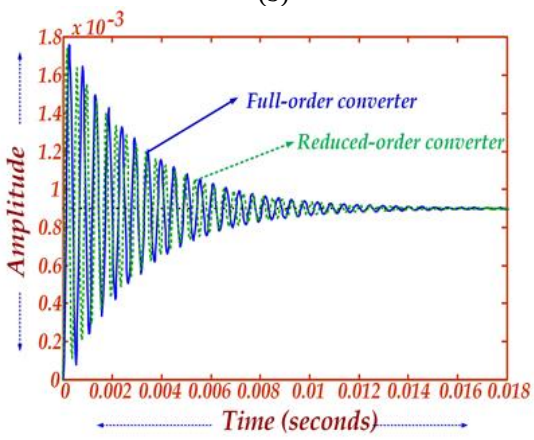

(c)

Fig. 8. Dynamic responses of full-order and reduced-order converter (a) Bode plot (b) Pole-zero map (c) Step response

Finally, to validate the accuracy of reduced-order modelling technique with power converter, time-domain and frequency-domain responses are obtained and presented in Fig 8. Fig 8 (a) and (b) presents the comparison of bode and pole-zero of original and reduced-order model. Similarly, the time-domain response is also obtained and it is depicted in Fig 8 (c).

6. Voltage gain and Efficiency analysis

6.1 Voltage gain comparison

Last decade several high gain topologies are reported in the literature [32-41]. In this section, the voltage gain of the HGSIC converter is compared with the topologies in [32-35]. From this comparative study, it is noted that the proposed topology's voltage gain is high compared to other topologies [32-35] for the duty cycle 0.2-0.8. Fig 9 depicts the comparative study carried out on HGSIC converter.

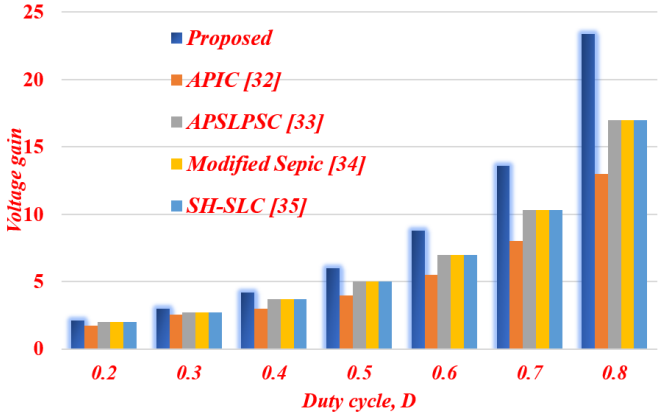

Fig. 9. Comparison of voltage gain versus Duty cycle, D

6.2 Efficiency analysis

The efficiency of the converter is determined by calculating the losses across the components of HGSIC converter.

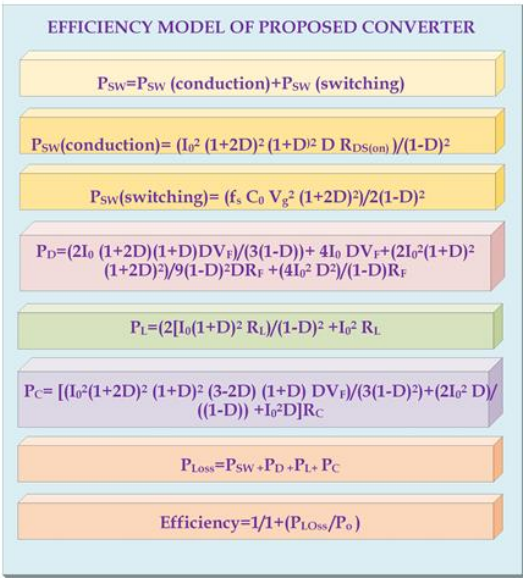

Fig. 10. Loss equations of components in HGSIC converter

Fig. 10 shows the equations for loss analysis of the HGSIC converter. The internal resistance of the switch is $R_{DS(ON)}$. The forward voltage drop of diode is V_F and the forward resistance is R_F. By determining the losses across these components, the efficiency of the converter is determined.

7. Results and discussion

From Fig 8 (c), it is well-known that both the time-responses are closely matching and it evidences the application of pole clustering techniques to high gain dc-dc converters. As shown in Fig 9, the voltage gain of the converter is compared and it is noted that the converter has high gain compared to topologies taken for the comparison. It is also observed that this technique is more easier and less computing compared other techniques because it can be computed with any software. In this article, entire analysis is carried out with Matlab software.

From this study, it is experiential that pole clustering technique is more suitable for power converters in mathematical modelling. It is also prominent that this technique will definitely ease the mathematical modelling of power converters for dynamic study and to design the controller for closed-loop operation.

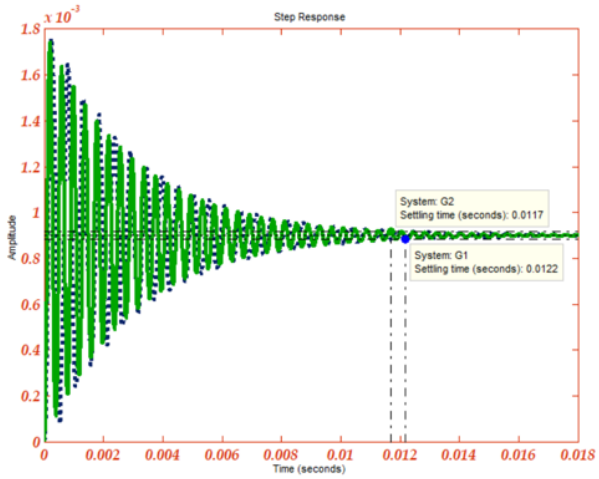

Fig. 11. Loss equations of components in HGSIC converter

Fig 11 shows the comparison between the full order and reduced order transfer function of the converter and the validation of pole clustering technique. Further, the applied technique is proved by presenting Table 5 which depicts the time domain parameters obtained from both full order and reduced order transfer functions of HGSIC converter.

Table 5. Time domain parameters Full order and reduced order HGSIC converter

System	Peak response	Settling time (Sec)	Rise time (sec)
Full order	95 %	0.012	7.0e-5
Reduced order	94 %	0.0117	6.7e-5

8. Experimental results

A 50 W prototype is tested for validating the performance of the topology. Fig 12 present the test results and photograph of the hardware setup. Fig 12 (a) present the input voltage of 12 V. The duty cycle is 0.35 and the gain of the converter is 3.53 times of the input voltage. The output voltage of 42 V as pulses is presented in Fig 12 (b). Fig 12 (c) depicts the gate pulse from driver circuit which validates the 35 % duty cycle.

Fig 12 (d) and (e) present the switch and diode voltage to validate the steady-state performance of the converter. Finally, the photograph of the laboratory prototype tested is presented in Fig 12 (f) along with digital storage oscilloscope taken for the output measurement. The gain of the converter is increased by increasing the number of switched inductor/ switched capacitor cell and without enhancing the duty cycle, D. This will reduce the power density of the converter. This proposed topology can be integrated with fuel cell powered source and it is more suitable because the input current is continuous and ripple-free.

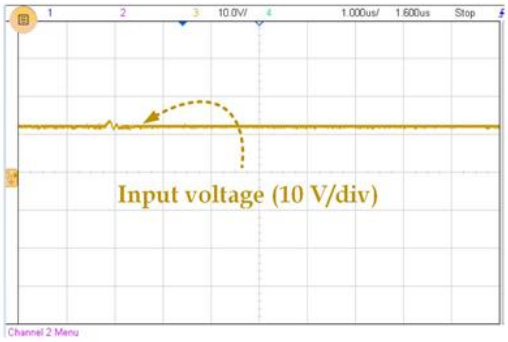

(a)

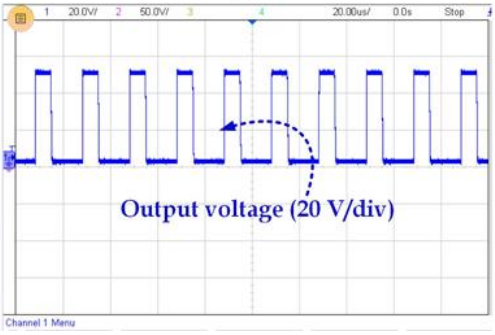

(b)

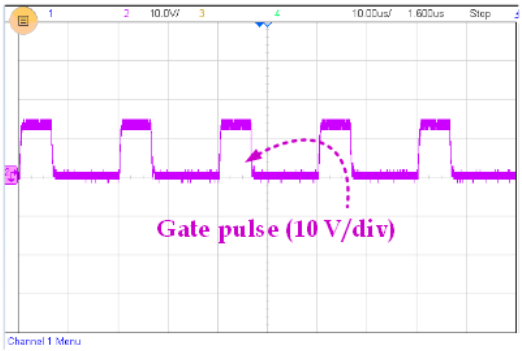

(c)

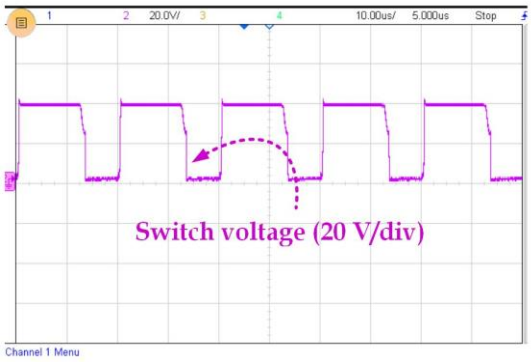

(d)

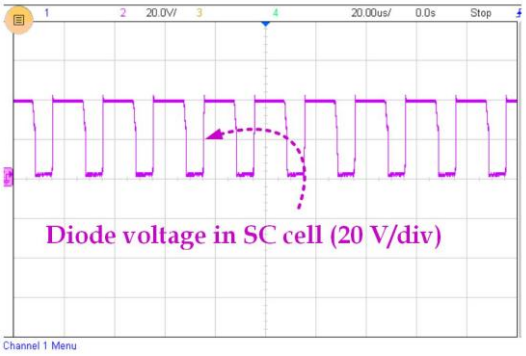

(e)

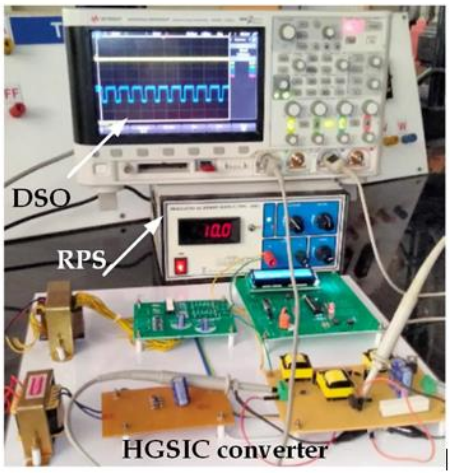

(f)

Fig. 12. Test results (a) Input voltage (b) Output voltage (c) Gate pulse (d) Switch voltage (e) Diode voltage (f) Photograph of HGSIC converter

9. Conclusion

HGSIC converter is tested and validated for the generation of high voltage gain and it is also observed that it can produce high voltage pulse. To perform the dynamic study, transfer function of the HGSIC converter is derived using switching flow graph modeling technique which is observed to be ease in computation compared to state space-averaging. Furthermore, to reduce the complexity in the design of controller, order reduction of the transfer function is performed with improved pole-clustering technique. The application of this technique to higher dimensional power converter is validated by obtaining the frequency and time-domain responses from MATLAB for HGSIC converter. A comparative study is performed with 4^{th} and 2^{nd} transfer function of the chosen converter. The results show that the improved pole-clustering technique is well suited for the suggested HGSIC converter. The validation of pole clustering technique is done and it is observed that the time domain parameters are closely matching. For example, the peak overshoot of full order and reduced order transfer function is 95 and 94 % respectively.

The voltage gain of the converter is compared with the similar topology in the literature and it is observed that the converter gives a gain of 14 for 0.7 duty cycle wheras other topologies produce the voltage gain of ≤ 10. Finally, a 50 W prototype is developed to validate the steady-state performance of HGSIC converter. As a future scope, a fault-tolerant topology with redundant switch and output capacitor can be proposed which will increase the reliability of the system. The reliability of the converter can be studied by determining the failure rate of the components in the converter. This analysis can be carried out using Military Handbook-217. If the topology is reconfigured with the fault-tolerant structure, the reliability of the system will be improved and which in turn reduces the replacement cost of the converter. Derivation of fault-tolerant structure with reliability study is considered as future scope of this work.

References

[1] S. Das, P. Patnaik and R. Jha, "Model order reduction of high order LTI system using Genetic Algorithm," 2017 International Conference on Computer, Communications and Electronics (Comptelix), 2017, pp. 73-77, doi: 10.1109/COMPTELIX.2017.8003941.

[2] R. Singh, V. M. Mishra and J. Singh, "Model Order Reduction via Routh Hurwitz Array and Improved Pade Approximations," 2018 International Conference on Power Energy, Environment and Intelligent Control (PEEIC), 2018, pp. 755-758, doi: 10.1109/PEEIC.2018.8665590.

[3] D. Krokavec and A. Filasová, "H2 Norm Principle in Order Reduction of Discrete-time Systems," 2019 20th International Carpathian Control Conference (ICCC), 2019, pp. 1-6, doi: 10.1109/CarpathianCC.2019.8765951.

[4] S. Li, "Loop Reversal Rule in Block Diagram and Signal Flow Graph Manipulation," in IEEE Signal Processing Letters, vol. 19, no. 10, pp. 672-675, Oct. 2012, doi: 10.1109/LSP.2012.2211869.

[5] U. Bhatnagar and A. Gupta, "Application of grey wolf optimization in order reduction of large scale LTI sys-tems," 2017 4th IEEE Uttar Pradesh Section International Conference on Electrical, Computer and Electronics (UPCON), 2017, pp. 686-691, doi: 10.1109/UPCON.2017.8251132.

[6] P. Mohammadalizadeh, F. M. Shahir and M. Shabani, "Mathematical modeling and dynamic analysis of self-lift P/O Lou converter by means of signal flow graph," 2015 9th International Conference on Electrical and Electronics Engineering (ELECO), 2015, pp. 1097-1101, doi: 10.1109/ELECO.2015.7394632.

[7] S. Osowski, "Signal flow graphs for determination of higher order sensitivities of circuit functions," 2011 20th European Conference on Circuit Theory and Design (ECCTD), 2011, pp. 437-440, doi: 10.1109/ECCTD.2011.6043380.

[8] Su X, Wu L, Shi P, Song YD. H∞ model reduction of Takagi-Sugeno fuzzy stochastic systems. IEEE Trans Syst Man Cybern B Cybern. 2012 Dec;42(6):1574-85. doi: 10.1109/TSMCB.2012.2195723. Epub 2012 May 18. PMID: 22623431.

[9] Zhe Yan, Chao Zhang, Hong Zhao, Fei Fan, Shutao Che and Xiaoming Cui, "Approximation of large time delay for MIMO systems by using matrix Pade-type," 2011 Second International Conference on Mechanic Automa-tion and Control Engineering, 2011, pp. 108-111, doi: 10.1109/MACE.2011.5986869.

[10] Bin Yao; Qinhong Zheng; Jinhui Peng; Runeng Zhong; Wansong Xu; Tai Xiang; Xiuming Li., "Analysis of loaded cavity by FDTD technique combining with sum algorithm and Padé ap-proximation," 2011 Second International Conference on Mechanic Automation and Control Engineering, 2011, pp. 7173-7176, doi: 10.1109/MACE.2011.5988705.

[11] Saaki, Indranil & Babu, Chandra & Ch, Krishna Rao & Prasad, D. (2011). Integral square error minimization technique for linear multi-input and multi output systems. 2011 International Conference on Power and Energy Sys-tems, ICPS 2011. 10.1109/ICPES.2011.6156665.

[12] D. K. Sambariya and H. Manohar, "Model order reduction by integral squared error minimization using bat algorithm," 2015 2nd International Conference on Recent Advances in Engineering & Computational Sciences (RAECS), 2015, pp. 1-7, doi: 10.1109/RAECS.2015.7453413.

[13] DongYin Wang and Youtian Tao, "Computation for exponential matrix via restrictive pade approximation," 2012 IEEE Symposium on Electrical & Electronics Engineering (EEESYM), 2012, pp. 536-538, doi: 10.1109/EEESym.2012.6258712.

[14] V. P. Singh, P. Chaubey and D. Chandra, "Model order reduction of continuous time systems using pole clus-tering and Chebyshev polynomials," 2012 Students Conference on Engineering and Systems, 2012, pp. 1-4, doi: 10.1109/SCES.2012.6199028.

[15] R. Singh, V. M. Mishra and J. Singh, "Model order reduction via time moment modeling and clustering tech-nique," 2017 4th IEEE Uttar Pradesh Section International Conference on Electrical, Computer and Electronics (UPCON), 2017, pp. 638-641, doi: 10.1109/UPCON.2017.8251124.

[16] N. S. Tanwar, R. Bhatt and G. Parmar, "Order reduction of linear continuous time interval system using mixed evolutionary technique," 2016 International Conference on Advanced Communication Control and Computing Tech-nologies (ICACCCT), 2016, pp. 265-270, doi: 10.1109/ICACCCT.2016.7831643.

[17] Kumar, Parvendra & Chaudhary, Sunil. (2017). Novel approach in classical pade approximation. 667-670. 10.1109/CONFLUENCE.2017.7943235.

[18] Kumari, Abha & Vishwakarma, Dr. C.B. (2019). Order Reduction of Dynamic Systems by Using Renovated Pole Clustering Technique. 532-537. 10.1109/PEEIC47157.2019.8976689.

[19] G. Vasu, K. V. S. Santosh and G. Sandeep, "Reduction of large scale linear dynamic SISO and MIMO systems using differential evolution optimization algorithm," 2012 IEEE Students' Conference on Electrical, Electronics and Computer Science, 2012, pp. 1-6, doi: 10.1109/SCEECS.2012.6184732.

[20] [20] Jeng, S.-L.; Roy, R.; Chieng, W.-H. A Matrix Approach for Analyzing Signal Flow Graph. Information 2020, 11, 562. https://doi.org/10.3390/info11120562

[21] P. Verma, P. K. Juneja and M. Chaturvedi, "Various Mixed Approaches of Model Order Reduction," 2016 8th International Conference on Computational Intelligence and Communication Networks (CICN), 2016, pp. 673-676, doi: 10.1109/CICN.2016.138

[22] Navamani, Divya & Krishnasamy, Vijayakumar & Anbazhagan, Lavanya. (2016). Switching flow graph modelling of RRPP based DC-DC converter. Indian Journal of Science and Technology. 9. 10.17485/ijst/2016/v9i43/101862.

[23] Z. Hongying, S. Xiaojie, S. Yongduan and L. Xinxin, "Model reduction of T-S fuzzy systems with time-varying delays," 2015 34th Chinese Control Conference (CCC), 2015, pp. 1963-1966, doi: 10.1109/ChiCC.2015.7259932.

[24] M. Garg, "Model order reduction and approximation analysis for control system design," 2017 4th Interna-tional Conference on Signal Processing, Computing and Control (ISPCC), 2017, pp. 473-476, doi: 10.1109/ISPCC.2017.8269725.

[25] J. Cai and T. J. Brazil, "Padé-approximation-based behavioral modeling," 2013 IEEE MTT-S International Microwave Symposium Digest (MTT), 2013, pp. 1-3, doi: 10.1109/MWSYM.2013.6697491.

[26] S. Shah, P. Koralewicz, V. Gevorgian and L. Parsa, "Small-Signal Modeling and Design of Phase-Locked Loops Using Harmonic Signal-Flow Graphs," in IEEE Transactions on Energy Conversion, vol. 35, no. 2, pp. 600-610, June 2020, doi: 10.1109/TEC.2019.2954112.

[27] N. Sharma and C. B. Vishwakarma, "Dynamic system simplification using pole clustering and continued fraction expansion," 2017 International Conference on Multimedia, Signal Processing and Communication Technologies (IMPACT), 2017, pp. 1-4, doi: 10.1109/MSPCT.2017.8363881.

[28] L. Shuang, Y. Jinsong and T. Diyin, "A new multi-signal flow graph-based method and implementation for complex system diagnosis," 2015 IEEE 10th Conference on Industrial Electronics and Applications (ICIEA), 2015, pp. 57-61, doi: 10.1109/ICIEA.2015.7334084.

[29] Abbasi, Majid & Afifi, Ahmad & pahlavani, Mohamadreza. (2018). Signal Flow Graph Modelling of a Switch-ing Converter with Single Inductor Triple Output DC-DC Structure. IET Power Electronics. 11. 10.1049/iet-pel.2017.0289.

[30] Appikonda, Mohan & Kaliaperumal, Dhanalakshmi. (2020). Signal flow graph model and control of dual input boost converter with voltage multiplier cell. AEU - International Journal of Electronics and Communications. 125. 153345. 10.1016/j.aeue.2020.153345.

[31] D. Kwon and G. A. Rincon-Mora, "Operation-based signal-flow AC analysis of switching DC-DC converters in CCM and DCM," 2009 52nd IEEE International Midwest Symposium on Circuits and Systems, 2009, pp. 957-960, doi: 10.1109/MWSCAS.2009.5235925.

[32] Y. Tang, D. Fu, T. Wang and Z. Xu (2015). Hybrid Switched-Inductor Converters for High Step-Up Conversion. IEEE Transactions on Industrial Electronics, vol. 62, no. 3, pp. 1480-1490,doi: 10.1109/TIE.2014.2364797.

[33] H. Mashinchi Maheri, E. Babaei, M. Sabahi and S. H. Hosseini (2017). High Step-Up DC–DC Converter With Minimum Output Voltage Ripple. IEEE Transactions on Industrial Electronics, vol. 64, no. 5, pp. 3568-3575, doi: 10.1109/TIE.2017.2652395.

[34] S. A. Ansari and J. S. Moghani (2019). A Novel High Voltage Gain Noncoupled Inductor SEPIC Converter. IEEE Transactions on Industrial Electronics, vol. 66, no. 9, pp. 7099-7108, doi: 10.1109/TIE.2018.2878127.

[35] M. A. Salvador, T. B. Lazzarin and R. F. Coelho (2018). High Step-Up DC–DC Converter with Active Switched-Inductor and Passive Switched-Capacitor Networks. IEEE Transactions on Industrial Electronics, vol. 65, no. 7, pp. 5644-5654, doi: 10.1109/TIE.2017.2782239.

[36] Komarasamy R, Albhonso N, Gurusamy G. Order reduction of linear systems with an improved pole clustering. Journal of Vibration and Control. 2012;18(12):1876-1885, doi:10.1177/1077546311426592

[37] A. BELKAID, I. COLAK, K. KAYISLI and R. BAYINDIR, "Indirect Sliding Mode Voltage Control of Buck Converter," 2020 8th International Conference on Smart Grid (icSmartGrid), 2020, pp. 90-95.

[38] Abdelaziz Sahbani, Kamel Cherif, Kamel Ben Saad, “Multiphase Interleaved Bidirectional DC-DC Converter for Electric Vehicles and Smart Grid Applications,” Int. J. SMART GRID (ijSmartGrid), vol. 4, no. 2, pp. 80-87, 2020.

[39] S. F. Jaber, A. M. Shakir, “Design and simulation of a boost-microinverter for optimized photovoltaic system performance,” Int. J. SMART GRID (ijSmartGrid), vol. 5, no. 2, pp. 94–102, 2021.

[40] Linss T Alex, Subranhsu Sekhar Dash, Jaikrishna V and R.Sridhar, “ Design and analysis of push-pull-flyback Interleaved converters for photovoltaic system”, 6th International Conference on Renewable Energy Research and Applications, pp. 757-761, 2017.

[41] Ming-Tsung Tsai, Ching-Lung Chu, Wei-Cong Chen, “Implementation of a serial AC/DC converter with modular control technology”, 7th International Conference on Renewable Energy Research and Applications, pp. 245-250, 2018.